Ecological Indicators 178 (2025) 114058

Contents lists available at ScienceDirect

Ecological Indicators

journal homepage: www.elsevier.com/locate/ecolind

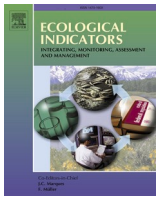

Original Articles

Microbial resistance and persistence increase during estuarine succession and promote nutrient accumulation

Songsong Gu [a,b,1], Xiongfeng Du [a,b,1], Mengting Maggie Yuan [c], Étienne Yergeau [d], Kai Feng [a], Zheng Zhang [e], Zhaojing Zhang [f], Yuqi Zhou [f], Linlin Wang [f], Danrui Wang [a,b], Tong Li [a,b], Chengliang Yan [a,b], Zhicheng Ju [a,b], Baohua Xie [g,h], Guangxuan Han [g,h], Ye Deng [a,b,*]

[a] CAS Key Laboratory for Environmental Biotechnology, Research Center for Eco-Environmental Sciences, Chinese Academy of Sciences, Beijing 100085, China
[b] College of Resources and Environment, University of Chinese Academy of Sciences, Beijing 100049, China
[c] Pacific Biosciences Research Center, University of Hawai'i at Mānoa, Honolulu 96822, United States
[d] Institut national de la recherche scientifique, Centre Armand-Frappier Santé Biotechnologie, 531 boul. des Prairies, Laval, Quebec, Canada
[e] Department of Marine Organism Taxonomy and Phylogeny, Institute of Oceanology, Chinese Academy of Sciences, Qingdao 266071, China
[f] Institute of Marine Science and Technology, Shandong University, Qingdao 266237, China
[g] Key Laboratory of Coastal Zone Environmental Processes and Ecological Remediation, Yantai Institute of Coastal Zone Research, Chinese Academy of Sciences, Yantai 264000, China
[h] Yellow River Delta Field Observation and Research Station of Coastal Wetland Ecosystem, Chinese Academy of Sciences, Yantai 264000, China

ARTICLE INFO

Keywords:
Microbial network
Temporal persistence
Topological resistance
Estuarine succession
Chronosequence

ABSTRACT

Understanding how belowground ecosystems maintain stability in the face of environmental change remains a fundamental challenge in ecology. In this study, we examined both the topological resistance and temporal persistence of microbial communities, including bacteria, fungi, and protists, across tidal and non-tidal zones in the Yellow River Delta (YRD), sampled across four seasons. Using amplicon sequencing, combined with molecular ecological networks and the iDIRECT framework, we found that succession from tidal wetland to non-tidal land significantly enhanced microbial diversity (average increase: 44.0 %) and temporal persistence (373.0 %), while simplifying network complexity (a 36.3 % reduction in intra- and inter-domain associations). Non-tidal land exhibited higher topological resistance and temporal persistence, indicating stronger ecological memory and reduced turnover. Multivariate analyses, including the Mantel test and structural equation modeling (SEM), confirmed that these changes were primarily driven by decreases in environmental stress (e.g., lower salinity and pH) and increases in soil nutrient accumulation (*i.e.*, soil organic matter and soil nitrogen). These results suggest that microbial relationships played critical roles in the succession of the estuary landscape. Our findings provide a practical basis for using microbial network stability as an indicator for ecological monitoring and management in various ecosystems.

1. Introduction

Ecosystems worldwide are under increasing pressure from both natural and anthropogenic disturbances, threatening their ability to maintain essential functions (De Keersmaecker et al., 2014; Pennekamp et al., 2018). Assessing ecosystem stability in the face of such pressures is critical, yet particularly challenging in natural habitats with limited aboveground biological indicators (Pennekamp et al., 2018). In such cases, microbial communities provide a promising alternative for monitoring ecosystem responses to change. Microorganisms are the most diverse and functionally significant life forms in soil, playing critical roles in organic matter decomposition, nutrient cycling, and energy flow (Angeloni et al., 2006; Li et al., 2021a). Recent studies have increasingly recognized microbial assemblages as sensitive bioindicators of environmental perturbations in aquatic and terrestrial systems (Ma et al., 2022). Thus, microbial stability may mirror the stability of the entire belowground ecosystem (Hernandez et al., 2021; Wu et al., 2021; Yuan et al., 2021).

* Corresponding author at: CAS Key Laboratory for Environmental Biotechnology, Research Center for Eco-Environmental Sciences, Chinese Academy of Sciences, Beijing 100085, China.
E-mail address: yedeng@rcees.ac.cn (Y. Deng).
[1] These authors contributed equally to this work.

https://doi.org/10.1016/j.ecolind.2025.114058
Received 13 May 2025; Received in revised form 23 July 2025; Accepted 13 August 2025
Available online 18 August 2025

Among the various aspects of ecosystem stability, three primary dimensions are often considered: (i) resistance, the state of staying essentially unchanged upon disturbance; (ii) resilience, the ability to return to the reference state after a temporary disturbance; and (iii) persistence (*opp.* variance), that describes the fluctuation of returning to the equilibrium across a time series (De Keersmaecker et al., 2014; Grimm and Wissel, 1997). While resistance and resilience have been widely studied, temporal persistence remains underexplored, particularly in the context of microbial communities. Persistence offers a dynamic measure of stability that captures how communities fluctuate or remain consistent across time under natural or anthropogenic stressors (Yuan et al., 2021). To quantify these dimensions of microbial stability, network theory has become an increasingly powerful tool. Microbial molecular ecological networks (MENs), adapted from concepts in food web theory, provide a structural framework for examining species interactions and the organization of communities (Deng et al., 2012; Dunne et al., 2002). Recent advances, such as iDIRECT, further enhance the reliability of inferred associations by distinguishing between direct and indirect relationships (Xiao et al., 2022). This study uses MENs to quantify both topological resistance (robustness and vulnerability) and temporal persistence (compositional stability, node persistence, and constancy of nodes and links).

Additionally, there is a long-standing debate regarding the relationship between community complexity and stability. Earlier theories suggested that more complex ecosystems with numerous species and interactions are more stable (MacArthur, 1955). In contrast, later models indicated that greater complexity may reduce stability due to increased sensitivity to perturbation and cascading effects (May, 1973). This question remains unresolved in microbial systems, which are inherently complex. Network-based metrics, such as average degree, clustering coefficient, geodesic distance, and cohesion, offer quantitative proxies for exploring this relationship in microbial ecology (Hernandez et al., 2021; Herren and McMahon, 2017).

Estuarine wetlands are ideal systems to study how microbial communities respond to environmental succession. The Yellow River Delta (YRD), shaped by sediment deposition and dynamic tidal action, is undergoing natural landscape succession, transitioning from tidal salt marshes to non-tidal vegetated lands, with seaward advancement at a rate of approximately 0.15 km/year (Fang et al., 2005). These contrasting environments provide an opportunity to assess how microbial communities respond to environmental filtering and ecological stabilization over time (Zhang et al., 2021).

In this study, we assessed the composition, structure, complexity, and stability of bacterial, fungal, and protistan communities in both tidal and non-tidal zones across four seasons. We specifically emphasize the role of temporal persistence as a core dimension of microbial stability. Our objectives were to test the following hypotheses: (i) estuarine succession significantly alters microbial diversity and increases temporal and topological stability; (ii) changes in stability are linked to shifts in community diversity and interaction complexity; and (iii) microbial stability correlates with increased soil nutrient accumulation. While some of these relationships are known (e.g., diversity correlates with stability, or nutrient-rich soils harbor more microbes), we aim to provide novel insights by disentangling the interactions among diversity, complexity, and persistence using integrated ecological network and statistical modeling approaches. Therefore, this study aims not only to examine how estuarine succession shapes microbial communities, but also to investigate how microbial stability may contribute to nutrient accumulation, forming a potential feedback loop between biotic structure and abiotic processes.

2. Materials and methods

2.1. Site characterization

The sampling sites (tidal wetland 37°47′14.496″N, 119°09′58.347″E; non-tidal land 37°45′59.36″N, 118°56′56.14″E) are located in the Yellow River Delta (YRD), along the southern shore of the Bohai Sea and the western Laizhou Bay, China. The YRD experiences a warm-temperate and continental monsoon climate, and is characterized by extensive saline and wet soils (Fig. 1a). Both the tidal wetland (initial stage) and the non-tidal land (succession states) were located within the core area of the Yellow River Delta National Nature Reserve. These zones are strictly protected and represent undisturbed natural habitats, with no evidence of land utilization or anthropogenic activities during the study period. The distance from the tidal wetland sampling site to the non-tidal land sampling site was about 19 km. The annual average temperature is 12.9 °C, with January's lowest and July's highest mean daily temperatures of −2.8 °C and 26.7 °C, respectively. The average annual precipitation is 560 mm. The soil type, ranging from tidal wetland to non-tidal land in the YRD, eventually changed from fluvo-aquic to saline soil, with the primary soil types identified as Calcaric Fluvisols, Gleyic Solonchaks, and Salic Fluvisols (FAO) (Han et al., 2015). The major vascular vegetation species for tidal and non-tidal zones were *Suaeda salsa* (L.) Pall. and *Phragmites australis* (Cav.) Trin. ex Steud., respectively (Zhao et al., 2020). This study employs a chronosequence approach (*i.e.*, space-for-time substitution), where spatially distinct sites representing different stages of estuarine succession, tidal wetland and non-tidal land, are compared to infer successional dynamics (Zaplata et al., 2013).

2.2. Sample collection

Soil samples were collected from two habitats (tidal wetland and non-tidal land) across four seasons, as autumn (2019-sep-21), winter (2020-Jan-4), spring (2020-Apr-7), and summer (2020-Jul-5) following a nested design within an 8 km^2 area (Fig. 1b), in which smaller sample regions are nestled inside bigger ones (Li et al., 2021b; Li et al., 2022). We used a soil auger with a 5 cm inner diameter, which was able to collect samples to a depth of 20 cm. For each season, 70 soil samples (tidal wetland, 37 samples; non-tidal land, 33 samples) were collected, where each sample was a composite of five replicates collected within a square meter area. In total, 280 soil samples (70 samples per season) were obtained. All samples were divided into two halves, one of which was maintained at 4 °C for the measurement of physicochemical characteristics, and the other at −80 °C for DNA extraction.

2.3. Soil physicochemical analyses

As previously mentioned, measurements of the soil moisture, pH value, salinity, total organic matter (OM), total nitrogen (TN), ammonia–nitrogen (NH_4^+-N), and nitrate nitrogen (NO_3^--N) contents in each soil sample were conducted (Du et al., 2021). In detail, moisture was determined by freeze-drying for 48 h. The salinity of the soil was quantified as electrical conductivity using a 1:2.5 soil-to-water ratio with a salinity meter (PAL-06S, ATAGO), and the pH was measured using a glass electrode (FiveEasy, METTLERTOLEDO). Total nitrogen (TN) and total phosphorus (TP) were determined using the alkaline potassium persulfate digestion method (K_2SO_8), followed by colorimetric detection with a UV–Vis spectrophotometer (UV-2550, SHIMADZU) (De Borba et al., 2014). Ammonium nitrogen (NH_4^+-N) and nitrate nitrogen (NO_3^--N) were extracted using 2 M KCl and measured using UV spectrophotometry following standard protocols. OM was measured by the K2CrO7 oxidation-colorimetric method.

2.4. DNA extraction, PCR amplification, and sequencing

Soil total DNA was extracted from 0.5 g of mixed soil using the Mobio DNeasy® PowerSoil® Kit. Universal primers were used to amplify the 16S rRNA genes of bacteria (515F: 5′-GTGCCAGCMGCCGCGGTAA-3′, 806R: 5′-GGACTACHVGGGTWTCTAAT-3′), ITS genes of fungi (5.8F: 5′-AACTTTYRRCAAYGGATCWCT-3′, 4R: 5′-

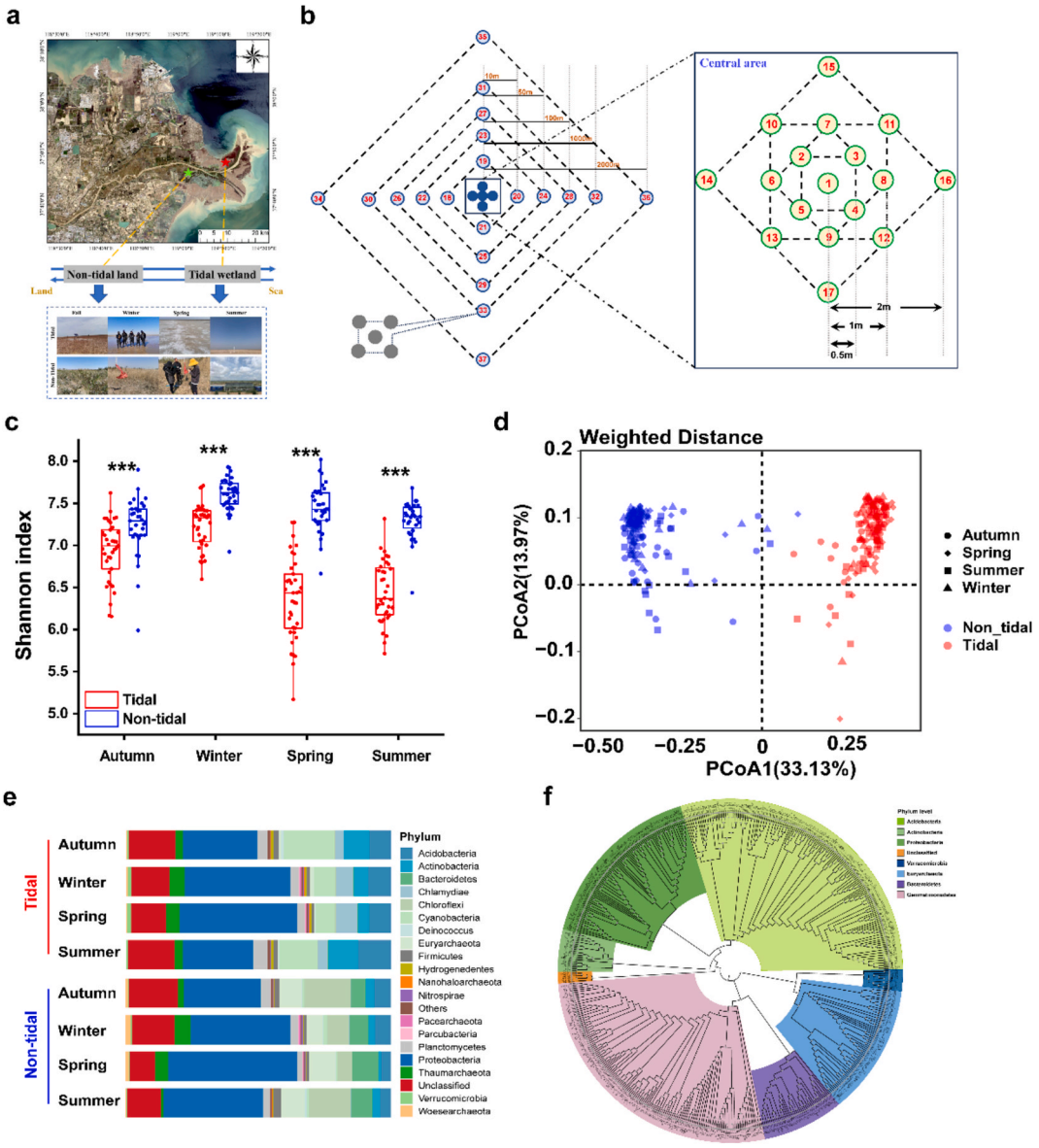

Fig. 1. Seasonal and tidal zone variations in microbial communities. (a) Overview of the sampling area. (b) Nested design of central sampling area and total sampling area. (c) Shannon index of bacterial diversity across different seasons (Autumn, Winter, Spring, Summer) and tidal zones (Tidal wetland in red, non-tidal land in blue). Significant differences in bacterial diversity are observed between tidal and non-tidal zones (*** $p < 0.001$). (d) Principal Coordinate Analysis (PCoA) plot of bacterial community based on weighted distance. Differed shape represents different seasons, while tidal wetland in red, non-tidal land in blue. (e) The relative abundance of major bacterial phyla in different seasons across tidal and non-tidal zone. (f) A phylogenetic tree of the bacterial community structure. The tree shows distinct groupings for different taxa, with colors indicating different phyla. (For interpretation of the references to color in this figure legend, the reader is referred to the web version of this article.)

AGCCTCCGCTTATTGATATGCTTAART-3′), and 18S genes of protistan (first step primer: 615F of 5′-AGTGTCGATTCGGTTAAAARGCTCGTAGTYG-3′, 963R of 5′-:AAGATCGTACTGAAGARGAYATCCTTGGTG-3′; second step primer: 615F of 5′-AGTGTCGATTCGGTTAAAARGCTCGTAGTYG-3′, 947R of 5′-AAGARGAYATCCTTGGTG-3′), and were supplemented with sample-specific barcodes (Caporaso et al., 2012; Yarza et al., 2014). PCR amplification was carried out in a total volume of 50 μL, consisting of 25 μL of 2 × Phusion High-Fidelity PCR Master Mix (New England Biolabs), 1 μM of each primer, and approximately 1 μL of template DNA (~10 ng). For bacterial 16S rRNA gene amplification (V4 region), the thermal cycling conditions included an initial denaturation at 98 °C for 30 s, followed by 30 cycles of denaturation at 98 °C for 10 s, annealing at 55 °C for 30 s, and extension at 72 °C for 30 s, with a final extension at 72 °C for 5 min. Fungal ITS region amplification was conducted under the following program: an initial denaturation at 95 °C for 3 min, followed by 35 cycles of 95 °C for 30 s, 55 °C for 30 s, and 72 °C for 45 s, and a final extension step at 72 °C for 10 min. Protistan 18S rRNA gene amplification involved a two-step nested PCR. The first round consisted of an initial denaturation at 95 °C for 3 min, followed by 25 cycles of 95 °C for 30 s, 57 °C for 30 s, and 72 °C for 45 s, with a final extension at 72 °C for 10 min. The second round used the same thermal cycling conditions with nested primers. All PCR products were examined on 2 % agarose gels, purified using AMPure XP beads (Beckman Coulter), and quantified before library preparation. Magigene Biotechnology Co., Ltd. (Guangzhou, China) sequenced the samples using the Illumina HiSeq platform with paired-end 2 × 150 bp read configuration.

2.5. Sequence processing

A total of 840 samples from the three microbial groups were

obtained. All raw reads from the 16S rRNA, ITS, and 18S genes were uploaded to a publicly accessible sequence analysis pipeline (https://dmap.denglab.org.cn/) that was integrated with multiple bioinformatics tools (Feng et al., 2024; Yang et al., 2024). First, the raw reads were allocated to samples based on their barcodes using the "Detected barcodes" tool, and then trimmed the barcode sequences. Second, The FLASH tool (Magoc and Salzberg, 2011) was used to combined forward and reverse reads, and the combined reads without ambiguous bases were filtered by using the Btrim tool (Kong, 2011). Then, the Greengene database (DeSantis et al., 2006), ITS RefSeq database (Schoch et al., 2014), and PR^2 database (Guillou et al., 2012) were used as references for chimera checking for the bacterial, fungal, and protistan communities, respectively. Singletons were preserved as uncommon species (Jousset et al., 2017), and sequencing clustering into operational taxonomic units (OTUs) was conducted at a 97 % threshold using UPARSE (Edgar, 2013). Moreover, for ITS gene sequences, the ITSx tool was used to identify ITS sequences and extract the ITS regions. After obtaining OTU tables, we randomly resampled the reads with 60,000, 25,000, and 30,000 sequences for per bacterial, fungal, and protistan datasets, respectively. The Ribosomal Database Project (RDP) classifier was used to assign bacterial, fungal, and protistan OTUs with the Greengene ribosomal database (Wang et al., 2007), UNITE database (Abarenkov et al., 2010) and PR^2 database (Guillou et al., 2012), respectively, with confidence values >0.8 (Wang et al., 2007).

2.6. Molecular ecological networks (MENs) and inter-domain ecological networks (IDENs) construction, characterization, and visualization

Random matrix theory (RMT) (Deng et al., 2012), the general framework iDIRECT and the Link Test for Environmental filtering or Dispersal limitation (LTED), were used to construct bacterial communities by Spearman correlation in the open-access analysis pipeline available at https://ieg4.rccc.ou.edu (Deng et al., 2012; Jizhong Zhou et al., 2010). Furthermore, inter-domain ecological networks (IDENs) based on the sparse correlations for compositional data (SparCC) method (Friedman and Alm, 2012), were constructed for bacterial-fungal, bacterial-protistan, and protistan-fungal networks through the open-accessible analysis pipeline available at https://inap.denglab.org.cn (Peng et al., 2024). All links, including inter- and intra-kingdom, were recovered, but only inter-kingdom links were retained. The Spearman correlations of RMT results of the bacterial community were filtered by the threshold $r > 0.78$, and SparCC results of bacterial-fungal, bacterial-protistan, and protistan-fungal communities were filtered by the thresholds $r > 0.5$, >0.6, and >0.4, respectively, and a false discovery rate < 0.05. Gephi (0.9.2) was used to display all the resulting networks. Due to the high dominance of a few taxa in the fungal and protistan datasets, where over 60 % of the total sequences were contributed by the top 20 OTUs, the number of nodes retained for network construction fell below the minimum threshold (*i.e.*, fewer than 50 nodes per network after prevalence filtering at a 0.5 occurrence rate). As a result, co-occurrence networks could not be reliably constructed for fungal and protistan communities using the RMT-based approach. Therefore, ecological networks based on molecular ecological network analysis (MENA) and iDIRECT were constructed only for the bacterial communities.

For MENs, various network topological indices were measured to characterize the topological structure (Deng et al., 2012), such as nodes, links, power-law fitting of node degrees, average degree (avgK), density (D), average clustering coefficient (avgCC), average path distance (GD), geodesic efficiency (E), harmonic geodesic distance (HD), transitivity (Trans), connectedness (Con), modularity, and keystone and module numbers. For IDENs, for each number of two interacting communities' species and total links, the connectance, cluster coefficient, web asymmetry, number of compartments, nestedness, checkerboard score, modularity, and specialization asymmetry were calculated (Feng et al., 2019). For each observed MEN and IDEN, the Maslov-Sneppen approach was used to generate 100 randomly rewired networks (Bascompte et al., 2003), and the topological properties of each of the 100 random IDENs were examined for each index. Importantly, cohesion, a powerful method for measuring the degree of cooperative behaviors or competitive interactions correlation (Herren and McMahon, 2017), which can indirectly represent the complexity, was used. While robustness (Dunne et al., 2002; Montesinos-Navarro et al., 2017), vulnerability (Deng et al., 2012), node and links constancy (Hautier et al., 2014), compositional stability (Tamara Jane Zelikova et al., 2014), and node persistence (Landi et al., 2018) were powerful indices to measure microbial stability (Yuan et al., 2021).

2.7. Microbial stability and complexity

Robustness (Dunne et al., 2002; Montesinos-Navarro et al., 2017) and vulnerability indices were used to evaluate community resistance. Robustness was calculated using the following two steps: First, the abundance-weighted mean interaction strength of node i ($wMIS_i$) was calculated using the equation below.

$$wMIS_i = \frac{\sum_{j \neq i} b_j s_{ij}}{\sum_{j \neq i} b_j} \tag{1}$$

Where b_j is the relative abundance of species j and s_{ij} is the association strength between species i and j, which is measured by the Pearson correlation coefficient. Second, nodes having $wMIS_i$ values of 0 were eliminated from the network, and finally, the fraction of remaining nodes was reported as the network robustness. And, the vulnerability was calculated by the following equation.

$$max\left(\frac{E - E_i}{E}\right) \text{ and } E = \frac{1}{n(n-1)} \sum_{i \neq j} \frac{1}{d_{ij}} \tag{2}$$

Where E represents global efficiency, E_i represents global efficiency after removing node i and all of its links, n represents the total number of nodes, and d_{ij} represents the shortest path between node i and j.

The indices of compositional stability, node persistence, node constancy and links constancy (Cang and Melodie, 2014; Yuan et al., 2021) were used to calculate the community persistence (Landi et al., 2018), which could be measured by the equations:

$$\text{Compositional stability} = \sqrt{\frac{\sum_{k=1}^{s} v(\min_{i} y_{i,k})}{\sum_{k=1}^{s} \sum_{i=1}^{v} y_{i,k}}} \tag{3}$$

and

$$\text{Node persistence} = \frac{\sum_{k=1}^{s} \prod_{i=1}^{v} \delta_{i,k}}{S} \tag{4}$$

Where v is the number of samples taken from the same field plot at multiple consecutive time points, S is the total species number of the network, $y_{i,k}$ is the abundance of species k in sample I, and $\delta_{i,k}$ is a Dirac delta function evaluating whether species k present in sample i. Node and links constancy (Cang and Melodie, 2014; Yuan et al., 2021) were defined as:

$$\text{Node constancy} = \frac{\mu_i}{\sigma_i} \tag{5}$$

and

$$l_{ij(+/-)} = \frac{\mu_{l_{ij(+/-)}}}{\sigma_{l_{ij(+/-)}}} \tag{6}$$

Where l_{ij} was the link of node i and j, the +/- mean the positive/negative correlation between node i and j. The μ_i and $\mu_{l_{ij}}$ were the mean abundance of node i and links l_{ij} across different sampling time point. The σ_i and $\sigma_{l_{ij}}$ were the standard deviation of abundances of node i and links l_{ij}

across different sampling time point.

In addition, we used the cohesion index to calculate network complexity, which was a null model-corrected metric considering abundance-weighted based, and could quantify the degree of connectivity. Positive and negative cohesion, which are all obtained from pairwise correlations, may show the degree of cooperative or competitive behavior in a sample of community members. Negative correlations might emerge from competition among species representing dissimilar niche needs (Freilich et al., 2018; Zelezniak et al., 2015), whereas positive correlations can be induced by facilitation/mutualism among taxa showing ecological or functional similarities (Barberán et al., 2012; Durán et al., 2018). The following equations were used to compute two cohesion values (positive and negative):

$$c_j^{pos} = \sum_{i=1}^{n} a_i \bullet \bar{r}_{i,r} > 0(PositiveCohesion) \quad (7)$$

and

$$c_j^{neg} = \sum_{i=1}^{n} a_i \bullet \bar{r}_{i,r} < 0(NegativeCohesion) \quad (8)$$

Where a_i is the abundance of OTU i in the sample j and $\bar{r}_{i,r}$ is the connectedness.

2.8. Statistical analysis

Every statistical analysis was also carried out using the analytic pipeline https://dmap.denglab.org.cn. To evaluate the richness of microbial communities, two indices of alpha-diversity were computed. To be more specific, the resampled OTU table's observed species counts were counted to calculate the Richness index, and Phylogenetic diversity was calculated after selecting the OTUs both in the tree file and OTU table. Locally weighted scatterplot smoothing (LOESS) was applied to visualize site-specific seasonal dynamics, implemented via "geom_smooth ()" in the "ggplot2" R package (v3.4.2). To quantify the strength and significance of monotonic seasonal associations, Spearman's rank correlation coefficients (ρ) were calculated for tidal and non-tidal zones separately using the "stat_cor ()" function from the "ggpubr" package (v0.6.0). The Mantel test determined the relationship between microbial communities and soil characteristics. The community's dissimilarity was tested using MRPP, ANOSIM, and PERMANOVA (Anderson, 2001). By ensuring the normal distribution, the differences in soil physicochemical variables and diversities between two habitats across four seasons were tested using the analysis of variance (ANOVA) implemented through the least significant difference (LSD) test, and Tukey post-hoc tests. The significance of link constancy and network features was evaluated using a one-sample Student's *t*-test by comparing the observed values to the distribution of 100 randomized networks generated using the Maslov–Sneppen rewiring method. The number of randomizations (n = 100) was selected to ensure reliable estimates of the null distribution. Using AMOS 21.0 (Amos Development Corporation), a structural equation model (SEM) was constructed. The fit of the suitable model was judged by the χ^2 test ($P > 0.05$) (Bentler and Bonett, 1980; Marsh and Hocevar, 1985), Chi-Square Test *df* value ($df \leq 5$, indicating relatively good model-data fit in general) (Schumacker and Lomax, 2004), root mean square error of approximation (RMSEA) (≤0.05, indicating relatively exact fit) (Browne and Cudeck, 1992; MacCallum et al., 1996; McDonald and Ho, 2002), comparative fit index (CFI) (≥0.95, indicating relatively exact fit (Satorra and Bentler, 1988)), goodness of fit index (GFI) and adjusted goodness fit index (AGFI) (≥0.90, indicating relatively exact fit (Tanaka and Huba, 1985)), normed fit index (NFI) (≥0.90, indicating relatively exact fit (Bentler and Bonett, 1980)) and relative fit index (RFI) (≥0.90, indicating relatively exact fit (Bollen, 1986)).

3. Results

3.1. Seasonal variations in environmental conditions and spatial heterogeneity

Soil physicochemical properties showed significant differences between tidal and non-tidal zones across all four seasons, as determined by one-way ANOVA followed by Tukey's post-hoc tests ($P < 0.05$) (Fig. 2). Non-tidal land soils consistently had lower pH and salinity, but higher organic matter (OM) and total nitrogen (TN) contents. Seasonal variations were more pronounced in tidal wetlands, where TN peaked in autumn and dropped in winter (Spearman's rank correlation coefficient, $R = 0.22$, $P = 0.011$). In contrast, non-tidal land TN showed some seasonal fluctuations, but the statistical analysis revealed no significant year-round variation ($R = 0.08$, $P = 0.36$), indicating that TN levels remained relatively stable throughout the year. Ammonium nitrogen (NH_4^+-N) fluctuated significantly in both zones (*paired t*, $P < 0.05$), peaking in spring and declining in summer, likely driven by seasonal mineralization and plant uptake. Nitrate nitrogen (NO_3^--N) exhibited clearer seasonal dynamics ($P < 0.001$), with higher concentrations in spring and autumn. Organic matter (OM) content was higher in spring and lower in autumn in both zones, with stronger fluctuations in tidal wetlands ($R = 0.35$, $P < 0.001$) compared to non-tidal soils ($R = 0.29$, $P < 0.001$). Soil pH also varied seasonally in both zones ($P < 0.001$), highest in winter and lowest in summer. Salinity changes were more pronounced in tidal wetlands, reflecting stronger seawater intrusion (Fig. 2a).

The spatial structuring of environmental heterogeneity, assessed through distance-decay relationships (DDRs) of environmental variations, also showed clear seasonal and habitat-specific differences (Fig. 2b). In the non-tidal land, environmental dissimilarity exhibited relatively weak distance-decay patterns across all seasons, with the slope of the relationship (β) ranging from 0.0479 to 0.159, and the explanatory power (R2) varying between 0.01 and 0.25. This suggests relatively homogeneous environmental conditions within the non-tidal land, with only weak spatial structuring. In contrast, the tidal wetland exhibited stronger and more seasonally variable distance-decay patterns. The steepest slope was observed in summer ($\beta = 0.163$), coupled with the highest explanatory power ($R2 = 0.32$, $P < 0.001$), indicating that spatial environmental heterogeneity was most pronounced during this season. In winter, although the slope ($\beta = 0.0375$) was lower, the distance-decay relationship remained statistically significant ($R2 = 0.03$, $P < 0.001$), highlighting the persistent spatial structuring driven by tides even under more homogeneous winter conditions. These results demonstrate that environmental factors in tidal wetlands not only undergo more pronounced seasonal fluctuations compared to non-tidal land, but also exhibit stronger spatial structuring, particularly during warmer seasons.

3.2. Succession-driven shifts in microbial diversity and composition

Microbial alpha diversity, as measured by the Shannon index, was consistently higher for bacterial and fungal communities in non-tidal land than in tidal wetlands across all seasons ($P < 0.05$), whereas protistan diversity remained relatively unchanged except in autumn (Fig. 1c; Fig. S1a, b). At the temporal scale, the proportion of the change for bacterial, fungal, and protistan communities within a year long time frame in non-tidal land (752.1, 103.43, and 9.975, respectively) was significantly lower ($P < 0.05$) than in tidal wetland (1083.7, 231.03 and 75.416, respectively). The above results indicated that wetland succession increased microbial community diversity and resistance to seasonal change. Beta diversity analyses (PCoA) revealed clear compositional separation between tidal and non-tidal zones, with fungal communities showing the strongest habitat-driven divergence (Fig. 1d; Fig. S2c-d). Along the first principal coordinate (PCoA1), tidal and non-tidal samples were distinctly separated across all community types, with the fungal

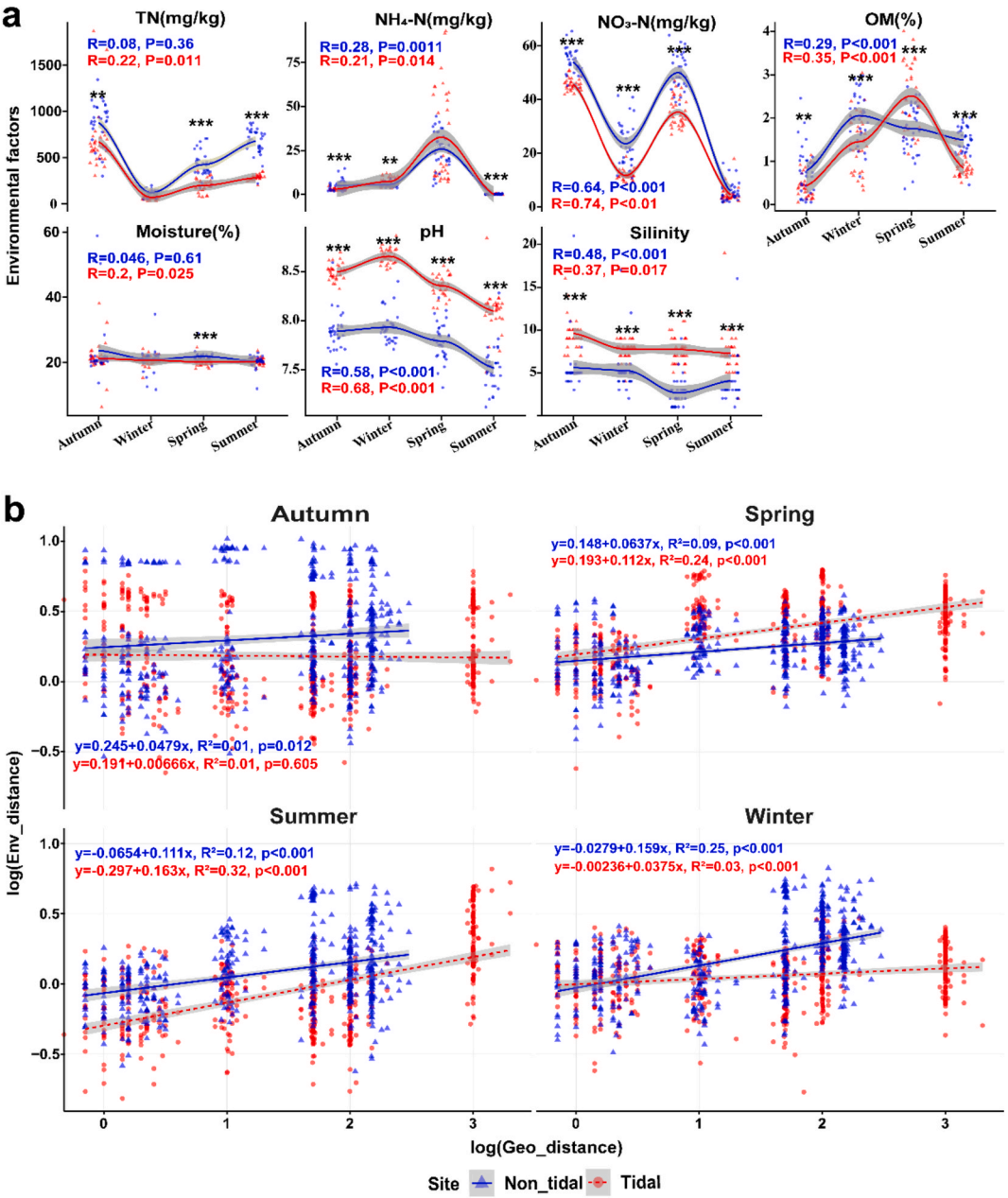

Fig. 2. Seasonal Patterns of Environmental Variables and Their Spatial Structuring in Tidal and Non-Tidal Wetlands. (a) Distribution of environmental factors across seasons (Autumn, Winter, Spring, Summer) and tidal zones (tidal wetland in red, non-tidal land in blue). Tidal wetland and non-tidal land are represented by orange and green, respectively. Asterisks indicate statistical significance between tidal and non-tidal zones (*, $P < 0.05$; **, $P < 0.01$; ***, $P < 0.001$). (b) Relationship between geographic distance (log-transformed) and environmental factors dissimilarity (log-transformed) for each season. Regression lines for tidal (red) and non-tidal (blue) zones are presented across the four seasons. (For interpretation of the references to color in this figure legend, the reader is referred to the web version of this article.)

community showing the most pronounced separation (explaining 33.4 % of the variation), followed by bacterial (33.13 %) and protozoan communities (28 %).

Across all seasons, Proteobacteria, Acidobacteria, and Actinobacteria dominated both tidal and non-tidal zones, with distinct habitat preferences (Fig. 1e). Non-tidal land harbored higher proportions of Acidobacteria and Verrucomicrobia, while Chloroflexi and Bacteroidetes were more enriched in tidal wetlands, highlighting the strong filtering effect of tidal regimes. Fungal communities were similarly shaped by habitat and seasonality (Fig. S2a). Ascomycota dominated across all seasons, with Basidiomycota and Chytridiomycota showing transient increases in tidal wetlands during spring and summer. Non-tidal land exhibited greater fungal compositional stability. Protistan communities (Fig. S2b) were largely dominated by Stramenopiles and Rhizaria, with tidal wetlands showing elevated Apusozoa and Archaeplastida, particularly in warmer seasons. Non-tidal land retained a simpler, more stable community structure. Phylogenetic analysis (Fig. 1f) revealed distinct clustering patterns between habitats, with taxa in non-tidal land forming tighter, more conserved lineages.

3.3. *Complexity and stability of bacterial community*

More than 60 % of the total sequences came from the top 20 OTUs in the fungal and protistan communities. Thus, each of the resulting community networks contained less than 50 nodes when the majority value of 0.5 was chosen for the whole community, and we were unable

to construct the ecological networks for fungal and protistan communities. Thus, only bacterial networks were constructed with the Molecular Ecological Network Approach (MENA) integrated with iDIRECT (Fig. 3a). Additionally, the contributions of environmental factors or dispersal limitation to the observed network links were disentangled by the Link Test for Environmental filtering or Dispersal limitation (LTED) that was further used to discard indirect associations caused by covariate patterns from environmental factors (Fig. 3b-e).

Multiple stability indices were calculated to elaborate on the effect of succession from tidal wetland to non-tidal land. The microbial temporal persistence, including compositional stability, node persistence, node constancy, and links constancy indices of the MENs were significantly higher ($P < 0.05$) in non-tidal land (Fig. 4a-d). Additionally, microbial topological resistance (e.g. vulnerability) was also, on average, significantly lower ($P < 0.05$) in non-tidal land (0.063 ± 0.029) than in tidal wetlands (0.156 ± 0.150) (Fig. 4e). Thereafter, the network topologies were measured. The range of average path lengths (GD) was 2.227 to 9.097, which was near the logarithm of the total number of nodes, indicating that all bacterial MENs possessed the characteristic small world. Since the empirical networks' modularity was much higher ($P > 0.05$) than the comparable randomized networks', these MENs seemed modular. Except for autumn, the tidal wetland networks possessed a higher avgK, D, avgCC, E, Trans and Con, and a smaller GD and HD, suggesting the tidal wetland had higher network complexity than non-tidal land (Table S1). Furthermore, the networks' scale (nodes and links), avgK, GD, Con, and number of keystone organisms and modules of the two habitats displayed a seasonal change. It was observed that the networks in winter and spring possessed a higher degree of complexity than in summer and autumn. We also calculated the cohesions value of communities to reflect the degree of cooperative behaviors or competitive interactions. The positive cohesion was observed to be significantly higher in tidal wetland than non-tidal land in autumn, winter, and summer, while a higher absolute value of negative cohesion was observed in tidal wetland in autumn and winter (Fig. 4f). In summary, wetland succession decreased the communities' complexity.

3.4. Microbial stability and complexity of the bipartite communities

To further discern the microbial existence pattern in these natural ecosystems, microbial IDENs (inter-domain ecological networks) were used to calculate the correlation of bipartite communities (*i.e.*, bacterial-fungal, bacterial-protistan, and fungal-protistan communities) in the two habitats across four seasons (Fig. S3). The bipartite networks also demonstrated certain fundamental network topological characteristics (Table S2, S3, and S4), such as nestedness and modularity. When observed and random IDENs were compared, nested structure, asymmetric specialization, and modularity were identified as nonrandom characteristics of the observed topological topologies for all bipartite networks at the local scale.

Some IDENs' properties (*i.e.,* connectance, cluster coefficient, and nestedness) presented the network complexity were listed as follows. The connectance (the proportion of the possible links observed as microbe-microbe associations) of bacterial-fungal, bacterial-protistan, and fungal-protistan communities' networks for all four seasons were, on average, all significantly lower ($P < 0.05$) in non-tidal land (0.036 ± 0.007, 0.042 ± 0.011 and 0.08 ± 0.049) than tidal wetland (0.07 ± 0.038, 0.08 ± 0.042 and 0.148 ± 0.096). Cluster coefficient (average cluster coefficient of all species) of the bacterial-protistan and fungal-protistan communities' networks in all four seasons were also, on average, significantly lower ($P < 0.05$) in non-tidal land (0.022 ± 0.014 and 0.05 ± 0.043) than tidal wetland (0.032 ± 0.023 and 0.123 ± 0.100), but the opposite trend was observed in bacterial-fungal community networks. The higher cluster coefficient of IDENs revealed a higher possibility of bacteria-fungi, bacteria-protist, and fungi- protist associations. The nestedness was used to measure the nested structure with a range from 0 (high nestedness) to 100 (chaotic structure). Significantly lower ($P < 0.05$) nestedness of the bacterial-fungal, bacterial-protistan, and fungal-protistan communities' bipartite networks in non-tidal land was observed for all four seasons (one-sample Student's *t*-test, $P < 0.001$). These basic properties of networks indicated that habitat succession could significantly decrease the complexity of bipartite communities.

The cohesion index was also used to calculate the complexity degree (*i.e.*, the degree of competition or cooperation) of bipartite communities. For bacterial-fungal communities, a significantly higher positive value of cohesion was observed in tidal wetland for spring and summer, while a higher absolute value of negative cohesion was also observed in tidal wetland in autumn, winter, and spring (Fig. S4). For bacterial-protistan communities, a significantly higher positive cohesion value was observed in tidal wetland in autumn, winter, and summer, while a higher absolute value of negative cohesion was observed in tidal wetland in autumn and winter. For fungal-protistan communities, a significantly higher value of positive cohesion was observed in tidal wetland in autumn and winter and non-tidal land in spring, while a higher absolute value of negative cohesion was observed in tidal wetland in winter. These cohesion analysis results indicated that the habitat succession could also significantly decrease the complexity degree of bipartite communities.

Also, we evaluated the influence of habitat succession on bipartite communities' stability. Multiple stability indices were computed using the empirical data to elaborate the effect of succession from tidal wetland to non-tidal land on bacterial-fungal, bacterial-protistan and fungal-protistan communities. The persistence property of stability including compositional stability, node persistence, node constancy, and links constancy were all observed to be significantly higher ($P < 0.05$) for the three bipartite communities in non-tidal land than tidal wetland (Fig. S5). The vulnerability index of community resistance in the four seasons possessed a significantly lower value ($P < 0.05$) in non-tidal land (Fig. S5d). And robustness index (the resistance of microbial networks to node loss) of community resistance possessed the significantly higher value ($P < 0.05$) in non-tidal land for the three communities in all four seasons (Table S5). Together these results indicated a significantly higher ($P < 0.05$) community temporal and topological stability after wetland succession.

3.5. Linking soil properties, microbial community, and microbial stability

A sub-community in our study was defined as a community that consisted of the OTUs which only observed within a network. The Mantel test, which is based on the Bray-Curtis distance, was employed to assess the link between soil characteristics and the sub-community. The results showed that, except for moisture, all measured soil properties significantly correlated with the sub-community of tidal wetland and non-tidal lands (Fig. 5a). TN, $NH4^{+}$-N, NO_3^{-}-N, OM, pH, and salinity were significantly correlated to the subcommunity of tidal wetland, while TN, NO_3^{-}-N, OM, pH, and salinity were significantly correlated to subcommunity of non-tidal land. These results showed that there were significant correlations between all networked communities with soil nutrients and environmental stress regardless of the coastal wetland habitat.

To evaluate the potential pathways linking environmental stress, soil nutrients, microbial communities, and network stability, we used structural equation modeling (SEM) for both bacterial and inter-domain sub-communities (Fig. 5b). Our model explained 97.95 % of the variance of total community diversity (*i.e.,* richness) 94.79 % of the variance in microbial stability (*i.e.,* compositional stability) and 46.9 % variance in microbial network complexity (*i.e.,* positive cohesion). Significant positive correlations of paths ($P < 0.001$) were found from salinity and pH value, which changed with the succession of wetland habitats to microbial communities' diversity and stability. However, significant positive interaction paths were found from pH value to network complexity, suggesting soil pH and salinity possessed a negative effect on microbial

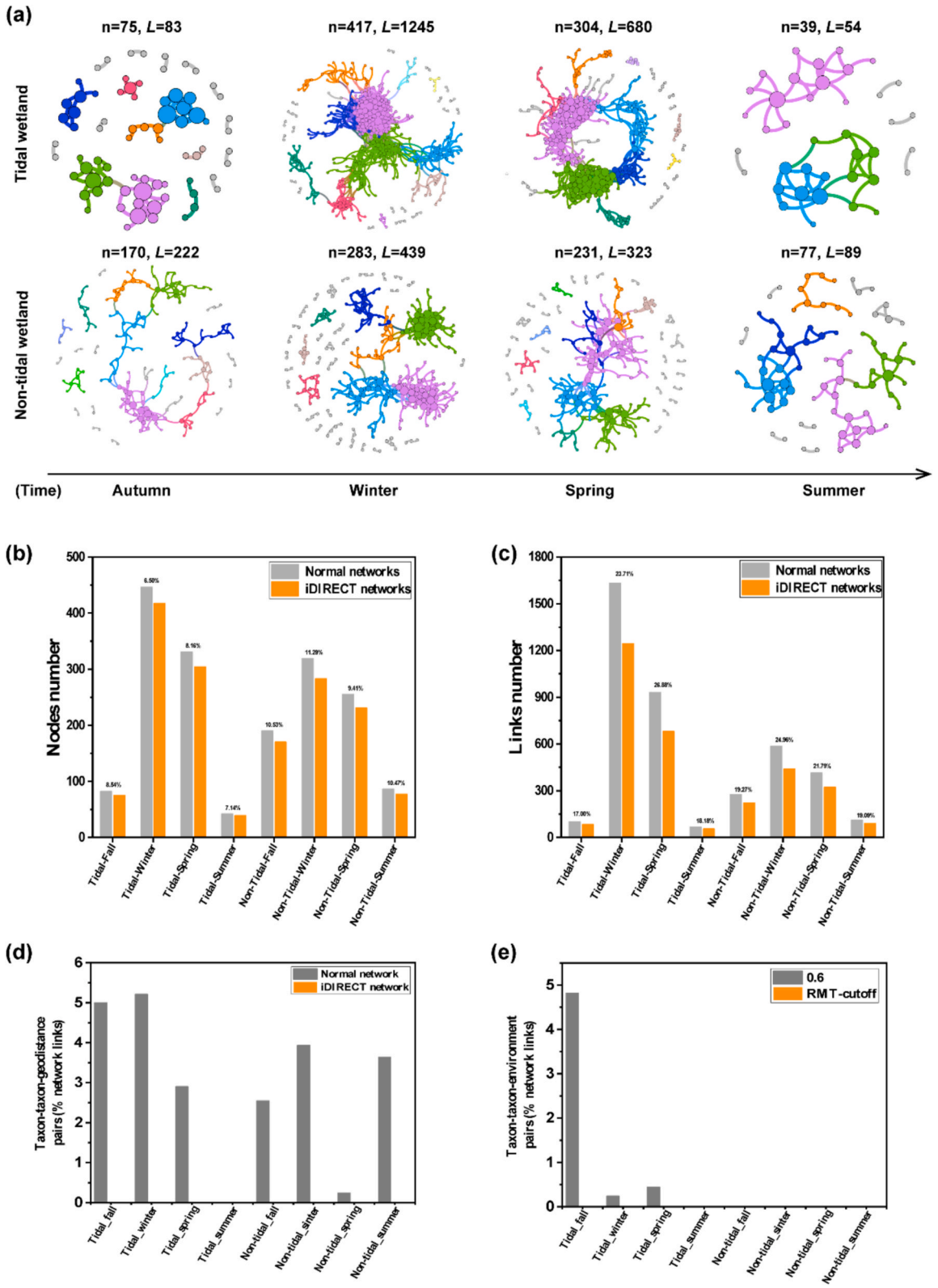

Fig. 3. Link Test for Environmental filtering or Dispersal limitation (LTED) for disentangling the contributions of environmental filtering or dispersal limitation to the observed network links, and disentangling direct associations from indirect associations between variables by a general framework through iDIRECT. (a) Tidal wetland and non-tidal land soil microbial RMT networks over time from fall to summer. Large modules, with ≥5 nodes, are shown in different colors, and smaller modules are shown in grey. L and n are links and nodes, respectively. The total numbers of nodes (b) and links (c) of normal and the reconstructed networks in the frameworks generated by iDIRECT and LTED with the same cutoff. The number above the bars is the percentage of removed nodes and indirect edges. (d) Potential taxon-taxon-geodistance links. The proportions of links in normal MENs and the MENs based on the framework in iDIRECT satisfying $p < 0.05$ with $r > 0$. (e) Potential taxon-taxon-environment links. We tested all taxon-taxon-environment links in all empirical iDIRECT MENs presented in this study. We used Spearman correlation and first set the correlation threshold $|r|$ equal to network correlation cutoff detected by RMT-based approach (0.78), while there was no links observed correlated to the environment factors.

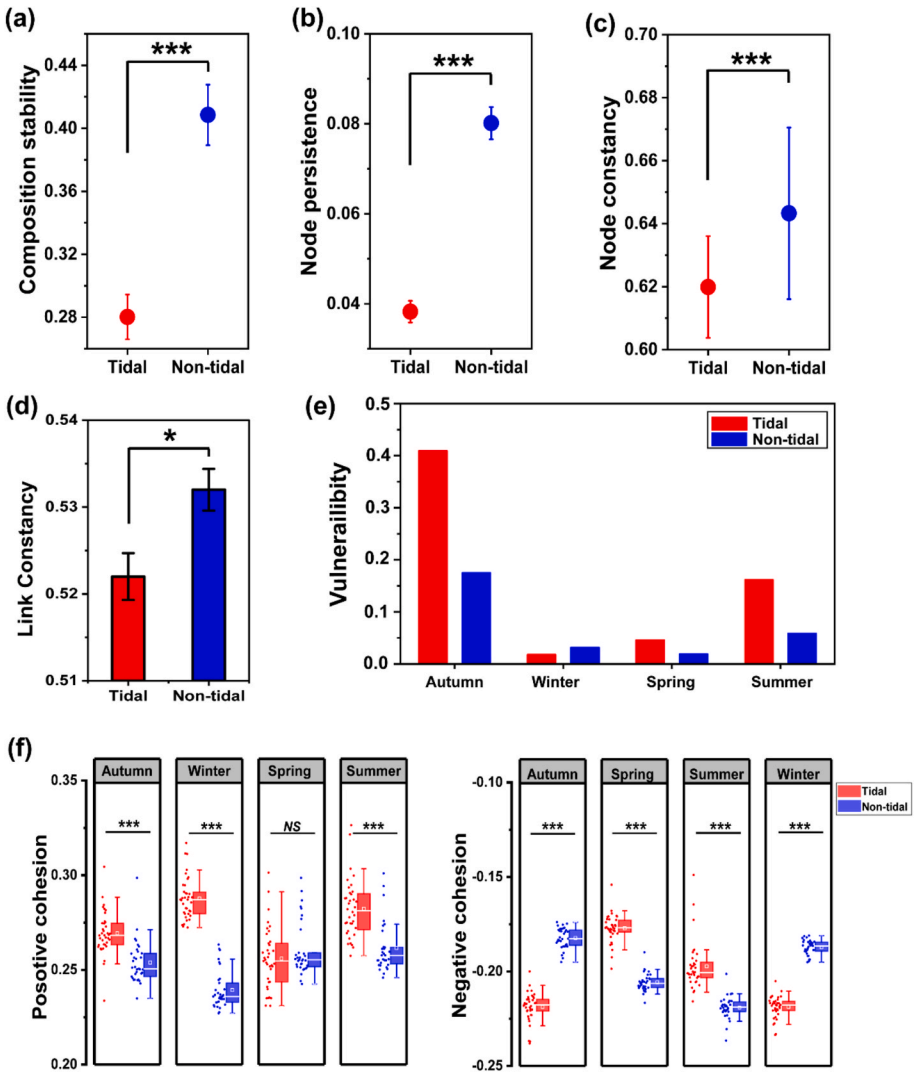

Fig. 4. Bacterial community topological resistance and temporal persistence. The compositional stability (a) and node persistence (b) of the network community over time from four adjacent seasons. Node (c) and link constancy (d) of the network community over time from four adjacent seasons. (e) Network vulnerability is measured by maximum node vulnerability in each network. Asterisks indicate the statistical significance. (f) The positive and negative cohesion values of the tidal and non-tidal communities. Box plots show inner quartiles and median positive and negative cohesion, while the detailed data are shown to the left side as points. Red and blue colors represent tidal wetland non-tidal land, respectively. X-axis represents the season from fall to summer. Asterisks indicate the statistical significance (*, $P < 0.05$; **, $P < 0.01$; ***, $P < 0.001$). (For interpretation of the references to color in this figure legend, the reader is referred to the web version of this article.)

community diversity and stability but a positive effect on network complexity. For the relationships among diversity, complexity and stability, the model revealed that the communities' diversity negatively influences the network complexity, and network complexity negatively influences the microbial stability. Furthermore, a significant positive correlation of path from microbial stability to TN and the significant positive interaction path from community diversity to OM were observed. These could reveal the role played by the microbiome during the succession of wetland habitats.

4. Discussion

In this study, we attempted to assess two aspects of microbial stability (*i.e.*, resistance and persistence) from two types of microbial ecological networks (*i.e.*, within and between microbial trophic levels) in a rapidly changing estuarine ecosystem (*i.e.*, tidal wetland and non-tidal land). Our results demonstrated some of the complicated relationships among diversity, complexity and stability, that support the notions that more diverse communities enhance ecosystem stability (MacArthur, 1955), and that lower complexity also increases the stability (Fan et al., 2018a; Jordán, 2009; Wu et al., 2021). Moreover, our results show that microbial communities, beyond passively responding to environmental changes, actively influence soil biogeochemistry. The reduction in salinity and pH during succession enhances microbial stability, which in turn promotes nutrient retention, creating bidirectional feedback that supports ecosystem development.

4.1. Microbial diversity increases as environmental stress is alleviated during estuarine succession

Natural estuarine succession phase, from tidal wetlands to inland non-tidal land, profoundly alters environmental conditions by mitigating external stressors such as tidal erosion, seawater intrusion, and seasonal salinity shifts. In the Yellow River Delta (YRD), this transition was associated with significantly reduced salinity and more neutral pH in non-tidal soils, consistent with previous reports on estuarine succession (Barbier et al., 2008; Murray et al., 2019). Our results confirm this pattern, showing that both salinity and pH were significantly lower in

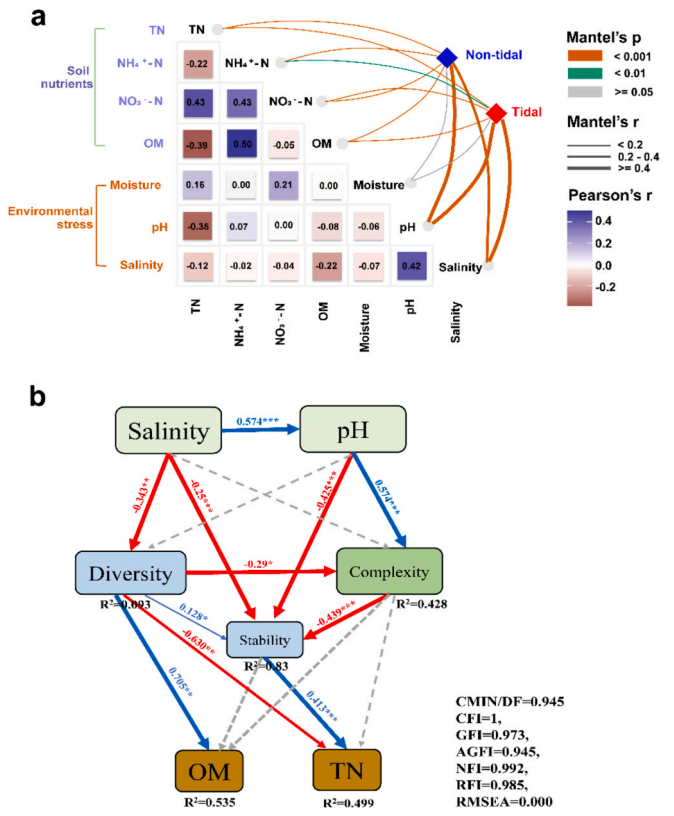

Fig. 5. Linkages Between Environmental Stress, Microbial Attributes, and Nutrient Accumulation in Wetland Succession. (a) Correlations between soil physicochemical properties and microbial communities. The bacterial community, based on Bray–Curtis distance, was related to each soil physicochemical property by Mantel test. Line width corresponds to the Mantel's r statistic, and line color denotes the statistical significance. Pairwise comparisons of environmental factors are also shown, with a color gradient denoting Pearson's correlation coefficient, and these factors were synthesized into two groups based on attribute of data surveyed. (b) Influence of wetland succession on the microbiome and soil nutrients by structural equation model (SEM). Diversity is represented by three types of community observed richness value, the network-stability is represented by three types of community intra and inter- kingdom networks' composition stability value, and complexity is represented by three types of community intra and inter- kingdom networks' positive cohesion value. Red lines represent negative correlations and blue lines represent positive correlations, while the width of lines is proportional to the degree of correlation. The proportion of variance explained by the response variable is shown alongside its variable and the goodness of fit for the SEM is shown beside the model. Asterisks indicate the statistical significance (*, $P < 0.05$; **, $P < 0.01$; ***, $P < 0.001$). (For interpretation of the references to color in this figure legend, the reader is referred to the web version of this article.)

non-tidal habitats across seasons (Fig. 2a), and their seasonal fluctuations were also attenuated (Fig. 2b), suggesting a more stable abiotic context. This environmental stabilization coincided with a marked increase in microbial alpha diversity, particularly for bacterial and fungal communities (Fig. 1c; Fig. 1a–b). Structural equation modeling (SEM) supported a mechanistic link, revealing significant negative effects of salinity and pH on microbial diversity (Fig. 5b). These findings indicated that alleviated environmental stress could promotes microbial colonization, survival, and niche differentiation (Gu et al., 2019; Wan et al., 2020; Zhang et al., 2021). Notably, while seasonal variation strongly influenced community structure, the rate of diversity change across seasons was lower in non-tidal habitats, indicating enhanced temporal consistency. This aligns with the notion that reduced stress fosters not only greater diversity but also more stable community (Shi et al., 2016; Yang et al., 2017).

4.2. Stress alleviation and the simplification of microbial networks

The progressive succession of estuarine wetlands was associated with a marked decline in the structural complexity of microbial co-occurrence networks, both within and across trophic levels. Intra-domain bacterial networks exhibited reductions in key topological properties, and similar trends were observed in inter-trophic networks, indicating that microbial interactions became sparser and less modular as succession progressed (Table S1) (Feng et al., 2022). These patterns align with the stress-gradient hypothesis (Bertness and Callaway, 1994), which posits that under high environmental stress, competitive interactions weaken while facilitative interactions become more prevalent (Hernandez et al., 2021). This shift is often attributed to the replacement of fast-growing competitive species with slow-growing, stress-tolerant taxa that are more likely to engage in cooperative or mutually beneficial interactions (Garcia et al., 2020; Männistö et al., 2016). Facilitative species, which provide direct benefits to neighboring community members, also tend to increase in abundance under stress conditions (Michalet et al., 2006). In tidal wetlands, higher salinity and pH fluctuations may impose physiological constraints on microbial survival, thereby promoting positive cohesion through cooperative or mutualistic interactions that enhance stress tolerance and metabolic complementarity. Conversely, in non-tidal land with more stable and nutrient-rich soils, the relaxed environmental filtering reduces the necessity for cooperation, and microbial taxa may increasingly compete for shared resources, leading to relatively lower positive cohesion and more neutral or competitive interactions. Consistent with this, we observed that positive cohesion values consistently exceeded negative cohesion across all seasons and for both intra- and inter-trophic networks, highlighting the dominance of positive associations in these wetland microbial communities (Hernandez et al., 2021). This reflects an ecological trade-off that cooperation dominates when stress mitigation is essential, while competition may increase when resources are abundant and niches overlap. The decline in network complexity with succession thus suggests that reduced environmental stress not only weakens competitive interactions but also diminishes the need for cooperative strategies, ultimately resulting in simpler microbial networks (Hernandez et al., 2021; Joshua E. Goldford et al., 2018; Piccardi et al., 2019). Structural equation modeling (SEM) further confirmed the link between environmental stress and network complexity, revealing a significant positive path from pH to network complexity (Fig. 5b). This provides direct evidence that harsher environmental conditions promote more complex and tightly connected microbial networks, as taxa are more reliant on mutualistic or facilitative relationships to persist under stress. Collectively, these results suggest that estuarine wetland succession, through the alleviation of salinity and pH stress, drives a fundamental restructuring of microbial networks, simplifying both intra-domain connectivity and cross-domain trophic interactions, while shifting community assembly processes from stress-driven facilitation to more environmentally relaxed competition.

4.3. Complexity-stability trade-offs in microbial networks

According to the "complexity weakens stability" theory, higher complexity negatively correlates with ecosystem stability (May 1973), because a more connected ecosystem could be more vulnerable due to cascade effects, through which one event triggers subsequent events and leads to amplification across the entire ecosystem (Deng et al., 2012; Helbing, 2013). This was later supported by studies showing that complexity could be negatively associated with microbial stability (Fan et al., 2018b; Jordán, 2009; Wu et al., 2021). One of the most striking findings in our study is the consistent and pronounced increase in microbial temporal persistence across estuarine succession (Fig. 4a-e; Fig. S5a-c). This trend was observed in both intra- and inter-domain microbial networks and persisted across all seasons. Temporal persistence, which reflects long-term compositional constancy and the ability

of communities to maintain structure through time (Montesinos-Navarro et al., 2017; Waldrop and Firestone, 2006), has received less attention compared to resistance and resilience in the literature. Yet, our results suggest that it is a particularly powerful and sensitive indicator of ecological stability in microbial systems, especially in chronically fluctuating or successional environments. Non-tidal land, characterized by reduced salinity and more neutral pH, exhibited higher compositional stability, node persistence, and constancy of nodes and links (Fig. 2a; Fig. 4). These indices suggest that microbial communities in non-tidal systems exhibit slower turnover and greater ecological memory, which may be indicative of increased niche specialization and resource coupling (Yang et al., 2010). Community diversity might be another factor that influences ecosystem stability. Given that greater diversity typically fosters community resistance to successional transitions (Naeem et al., 1994; Pimm, 1984; Tilman and Downing, 1994), the SEM revealed that diversity displayed a significantly positive interaction with microbial stability. This decline in cross-domain complexity may also reflect changes in specific ecological strategies under different stress regimes. For example, under high salinity in tidal wetlands, bacterial-fungal mutualisms, such as mycorrhizal-like symbioses or nutrient-sharing interactions, may be favored, as cooperative associations can enhance stress tolerance and metabolic flexibility (Berrios et al., 2023). However, as environmental stress is alleviated in non-tidal land, such selective pressures may diminish, reducing the ecological necessity of tight mutualistic relationships. This shift could explain the observed reduction in cross-domain link density and cohesion values in our IDENs, consistent with the idea that functional cooperation is more critical under harsher conditions, while relaxed environments promote more autonomous microbial strategies. Accordingly, the additional bacterial, fungal, and protistan community richness with wetland succession contributed to the observed increased stability of the non-tidal land microbial community. These changes of diversity and complexity bring about increasing stability of the community during estuary succession from tidal wetland to non-tidal land.

4.4. *Microbial stability played an important role in accumulating soil nutrients during estuary succession*

The interplay between microbial stability and ecosystem nutrient dynamics appears to be deeply intertwined and bidirectional (Zhou et al., 2012). SEM analyses revealed that reduced environmental stress enhanced microbial diversity and stability, which in turn positively affected soil nutrient levels, including soil organic matter and total nitrogen (Fig. 5a–b). These patterns are consistent with previous studies indicating that stable microbial networks, by virtue of reduced turnover and consistent activity, play a crucial role in promoting long-term carbon and nitrogen retention (Liang et al., 2017). In particular, we observed a significant positive path from microbial diversity to stability and from stability to nutrient accumulation in SEM results, suggesting a cascading effect whereby diverse communities stabilize microbial networks (Moore et al., 2005; Tilman et al., 2006), which in turn enhance nutrient deposition. This may be facilitated by more efficient trophic interactions, greater niche complementarity, and sustained metabolic pathways (Amyntas et al., 2023). These findings support the microbial carbon pump (MCP) hypothesis, which posits that microbial biomass and metabolic by-products can become long-lived carbon pools via the entombing effect (Jiao et al., 2024). Thus, increased microbial persistence in non-tidal lands may actively contribute to soil nutrient buildup. Conversely, elevated nutrient levels may also reinforce microbial stability (Kang et al., 2024; Usman et al., 2025). Soils with higher OM and TN can support richer and more resilient microbial communities by providing consistent energy and nutrient sources, buffering seasonal fluctuations (de Andrade Bonetti et al., 2017). Additionally, changes in nutrient status can feedback into community assembly and interaction strength, potentially reinforcing compositional stability. The reduced groundwater influence and tidal flushing in non-tidal lands may also contribute to the retention of soluble nutrients, further supporting this feedback loop (Han et al., 2015; Zhao et al., 2020). The vegetation shifts associated with succession from *Suaeda salsa* to *Phragmites australis*-dominated stands further reinforce this system. *P. australis* not only exhibits higher carbon sequestration capacity but also contributes more persistent organic inputs through litter deposition, which feeds microbial activity and reinforces long-term nutrient retention (Zhao et al., 2020). This vegetative feedback illustrates how microbial stability may not only reflect but also drive ecosystem maturation. Furthermore, the patterns observed in this estuarine system may extend to other aquatic ecosystems, such as lakes or inland wetlands, where succession and stress alleviation similarly shape microbial networks and nutrient retention (Guo et al., 2024; Guo et al., 2023). In these environments, stable microbial communities, buffered from tidal disturbances, can enhance soil biogeochemistry through sustained metabolic activity (Chen et al., 2022). Given the sensitivity of estuaries to anthropogenic stressors like nutrient runoff and hydrological alterations, future studies should also consider human impacts when evaluating microbial-nutrient feedbacks (Jennerjahn and Mitchell, 2013). Taken together, these findings support a dual mechanism: environmental filtering initiates microbial community stabilization, and stable microbial networks, in turn, shape nutrient cycling and support further environmental development. This bidirectional coupling between microbial persistence and nutrient dynamics represents a self-reinforcing loop fundamental to the progression of estuarine succession.

5. Conclusion

This study demonstrates that natural estuarine succession from tidal wetlands to non-tidal land enhances belowground microbial diversity and stability by alleviating environmental stress and simplifying interaction networks. Among the various stability metrics assessed, temporal persistence emerged as the most sensitive and integrative indicator of long-term microbial stability. Our findings reveal a clear trade-off that reduced network complexity and interaction intensity correspond with increased resistance and persistence. Importantly, we demonstrate that enhanced microbial persistence is associated with increased soil nutrient accumulation, highlighting a potential feedback loop in which stable microbial communities contribute to nutrient retention and cycling. This insight supports the microbial carbon pump hypothesis and underscores the ecosystem's functional relevance to microbial dynamics. By emphasizing temporal persistence as a central ecological property, this study refines the conceptual framework for evaluating microbial stability. This study demonstrates that natural estuarine succession from tidal wetlands to non-tidal land enhances belowground microbial diversity and stability by alleviating environmental stress and simplifying interaction networks. Among the various stability metrics assessed, temporal persistence emerged as the most sensitive and integrative indicator of long-term microbial stability. Our findings reveal a clear trade-off that reduced network complexity and interaction intensity correspond with increased resistance and persistence. Importantly, we demonstrate that enhanced microbial persistence is associated with increased soil nutrient accumulation, highlighting a potential feedback loop in which stable microbial communities contribute to nutrient retention and cycling. This insight supports the microbial carbon pump hypothesis and underscores the ecosystem's functional relevance to microbial dynamics. By emphasizing temporal persistence as a central ecological property, this study refines the conceptual framework for evaluating microbial stability. Moreover, our approach, linking microbial molecular ecological networks and iDIRECT-derived stability indices with soil nutrient dynamics, offers a quantitative and scalable tool for environmental monitoring. These indices could be integrated into long-term monitoring programs to detect early signs of ecosystem shifts and guide adaptive management in coastal and estuarine landscapes under increasing environmental pressures. These insights may inform restoration ecology and the management of coastal and estuarine

systems facing environmental change.

CRediT authorship contribution statement

Songsong Gu: Writing – original draft, Visualization, Software, Formal analysis, Data curation. **Xiongfeng Du:** Writing – original draft, Data curation. **Mengting Maggie Yuan:** Writing – review & editing. **Étienne Yergeau:** Writing – review & editing. **Kai Feng:** Writing – review & editing, Software, Formal analysis. **Zheng Zhang:** Data curation. **Zhaojing Zhang:** Formal analysis, Data curation. **Yuqi Zhou:** Data curation. **Linlin Wang:** Data curation. **Danrui Wang:** Data curation. **Tong Li:** Formal analysis, Data curation. **Chengliang Yan:** Formal analysis, Data curation. **Zhicheng Ju:** Formal analysis, Data curation. **Baohua Xie:** Resources. **Guangxuan Han:** Resources. **Ye Deng:** Writing – review & editing, Resources, Methodology, Funding acquisition.

Funding

This work was supported by the National Natural Science Foundation of China (U23A2043, 42277104).

Declaration of competing interest

The authors declare that they have no known competing financial interests or personal relationships that could have appeared to influence the work reported in this paper.

Acknowledgments

We thank Dr. James Walter Voordeckers for carefully editing the manuscript's grammar and for providing some valuable suggestions.

Declarations

This article does not contain any studies with human participants or animals performed by any of the authors.

Consent for publication

All authors have read and approved the manuscript. This work has not been published previously, nor is it being considered by any other peer reviewed journal.

Appendix A. Supplementary data

Supplementary data to this article can be found online at https://doi.org/10.1016/j.ecolind.2025.114058.

Data availability

The raw sequence data reported in this paper have been deposited in the Genome Sequence Archive in the National Genomics Data Center, China National Center for Bioinformation / Beijing Institute of Genomics, Chinese Academy of Sciences (GSA: CRA007306, CRA007308, CRA007309) and are publicly accessible at https://ngdc.cncb.ac.cn/gsa.

References

Abarenkov, K., Henrik Nilsson, R., Larsson, K.H., Alexander, I.J., Eberhardt, U., Erland, S., Høiland, K., Kjøller, R., Larsson, E., Pennanen, T., Sen, R., Taylor, A.F.S., Tedersoo, L., Ursing, B.M., Vrålstad, T., Liimatainen, K., Peintner, U., Kõljalg, U., 2010. The UNITE database for molecular identification of fungi – recent updates and future perspectives. New Phytol. 186, 281–285. https://doi.org/10.1111/j.1469-8137.2009.03160.x.

Amyntas, A., Berti, E., Gauzens, B., Albert, G., Yu, W., Werner, A.S., Eisenhauer, N., Brose, U., 2023. Niche complementarity among plants and animals can alter the biodiversity–ecosystem functioning relationship. Funct. Ecol. 37, 2652–2665. https://doi.org/10.1111/1365-2435.14419.

Anderson, M.J., 2001. A new method for non-parametric multivariate analysis of variance. Austral Ecol. 26, 32-46. 10.1111/j.1442-9993.2001.01070.pp.x.

Angeloni, N.L., Jankowski, K.J., Tuchman, N.C., Kelly, J.J., 2006. Effects of an invasive cattail species (Typha × glauca) on sediment nitrogen and microbial community composition in a freshwater wetland. FEMS Microbiol. Lett. 263, 86–92. https://doi.org/10.1111/j.1574-6968.2006.00409.x.

Barberán, A., Bates, S.T., Casamayor, E.O., Fierer, N., 2012. Using network analysis to explore co-occurrence patterns in soil microbial communities. ISME J. 6, 343–351. https://doi.org/10.1038/ismej.2011.119.

Barbier, E.B., Koch, E.W., Silliman, B.R., Hacker, S.D., Wolanski, E., Primavera, J., Granek, E.F., Polasky, S., Aswani, S., Cramer, L.A., Stoms, D.M., Kennedy, C.J., Bael, D., Kappel, C.V., Perillo, G.M.E., Reed, D.J., 2008. Coastal ecosystem-based management with nonlinear ecological functions and values. Science 319, 321–323. https://doi.org/10.1126/science.1150349.

Bascompte, J., Jordano, P., Melián, C.J., Olesen, J.M., 2003. The nested assembly of plant–animal mutualistic networks. PNAS 100, 9383–9387. https://doi.org/10.1073/pnas.1633576100.

Bentler, P.M., Bonett, D.G., 1980. Significance tests and goodness of fit in the analysis of covariance structures. Psychol. Bull. 88, 588–606. https://doi.org/10.1037/0033-2909.88.3.588.

Berrios, L., Yeam, J., Holm, L., Robinson, W., Pellitier, P.T., Chin, M.L., Henkel, T.W., Peay, K.G., 2023. Positive interactions between mycorrhizal fungi and bacteria are widespread and benefit plant growth. Curr. Biol. 33, 2878–2887.e2874. https://doi.org/10.1016/j.cub.2023.06.010.

Bertness, M.D., Callaway, R., 1994. Positive interactions in communities. Trends Ecol. Evol. 9, 191–193. https://doi.org/10.1016/0169-5347(94)90088-4.

Bollen, K.A., 1986. Sample size and bentler and Bonett's nonnormed fit index. Psychometrika 51, 375–377. https://doi.org/10.1007/BF02294061.

Browne, M.W., Cudeck, R., 1992. Alternative ways of assessing model fit. Sociol. Methods Res. 21, 230–258. https://doi.org/10.1177/0049124192021002005.

Cang, H., Melodie, A.M., 2014. Zeta diversity as a concept and metric that unifies incidence-based biodiversity patterns. Am. Nat. 184, 684–694. https://doi.org/10.1086/678125.

Caporaso, J.G., Lauber, C.L., Walters, W.A., Berg Lyons, D., Huntley, J., Fierer, N., Owens, S.M., Betley, J., Fraser, L., Bauer, M., Gormley, N., Gilbert, J.A., Smith, G., Knight, R., 2012. Ultra-high-throughput microbial community analysis on the Illumina HiSeq and MiSeq platforms. ISME J. 6, 1621–1624. https://doi.org/10.1038/ismej.2012.8.

Chen, Y.-J., Leung, P.M., Cook, P.L.M., Wong, W.W., Hutchinson, T., Eate, V., Kessler, A. J., Greening, C., 2022. Hydrodynamic disturbance controls microbial community assembly and biogeochemical processes in coastal sediments. ISME J. 16, 750–763. https://doi.org/10.1038/s41396-021-01111-9.

de Andrade Bonetti, J., Anghinoni, I., de Moraes, M.T., Fink, J.R., 2017. Resilience of soils with different texture, mineralogy and organic matter under long-term conservation systems. Soil Tillage Res. 174, 104–112. https://doi.org/10.1016/j.still.2017.06.008.

De Borba, B.M., Jack, R.F., Rohrer, J.S., Wirt, J., Wang, D., 2014. Simultaneous determination of total nitrogen and total phosphorus in environmental waters using alkaline persulfate digestion and ion chromatography. J. Chromatogr. A 1369, 131–137. https://doi.org/10.1016/j.chroma.2014.10.027.

De Keersmaecker, W., Lhermitte, S., Honnay, O., Farifteh, J., Somers, B., Coppin, P., 2014. How to measure ecosystem stability? An evaluation of the reliability of stability metrics based on remote sensing time series across the major global ecosystems. Glob. Chang. Biol. 20, 2149–2161. https://doi.org/10.1111/gcb.12495.

Deng, Y., Jiang, Y.H., Yang, Y., He, Z., Luo, F., Zhou, J., 2012. Molecular ecological network analyses. BMC Bioinf. 13, 113. https://doi.org/10.1186/1471-2105-13-113.

DeSantis, T.Z., Hugenholtz, P., Larsen, N., Rojas, M., Brodie, E.L., Keller, K., Huber, T., Dalevi, D., Hu, P., Andersen, G.L., 2006. Greengenes, a chimera-checked 16S rRNA gene database and workbench compatible with ARB. Appl. Environ. Microbiol. 72, 5069–5072. https://doi.org/10.1128/AEM.03006-05.

Du, X., Deng, Y., Li, S., Escalas, A., Feng, K., He, Q., Wang, Z., Wu, Y., Wang, D., Peng, X., Wang, S., 2021. Steeper spatial scaling patterns of subsoil microbiota are shaped by deterministic assembly process. Microb. Ecol. 30, 1072–1085. https://doi.org/10.1111/mec.15777.

Dunne, J.A., Williams, R.J., Martinez, N.D., 2002. Food-web structure and network theory: the role of connectance and size. PNAS 99, 12917–12922. https://doi.org/10.1073/pnas.192407699.

Durán, P., Thiergart, T., Garrido Oter, R., Agler, M., Kemen, E., Schulze Lefert, P., Hacquard, S., 2018. Microbial interkingdom interactions in roots promote arabidopsis survival. Cell 175, 973–983.e914. https://doi.org/10.1016/j.cell.2018.10.020.

Edgar, R.C., 2013. UPARSE: highly accurate OTU sequences from microbial amplicon reads. Nat. Methods 10, 996–998. https://doi.org/10.1038/nmeth.2604.

Fan, Y., Chen, S., Zhao, B., Yu, S., Ji, H., Jiang, C., 2018b. Monitoring tidal flat dynamics affected by human activities along an eroded coast in the Yellow River Delta, China. Environ. Monit. Assess. 190, 396. https://doi.org/10.1007/s10661-018-6747-7.

Fan, K., Weisenhorn, P., Gilbert, J.A., Chu, H., 2018a. Wheat rhizosphere harbors a less complex and more stable microbial co-occurrence pattern than bulk soil. Soil Biol. Biochem. 125, 251–260. https://doi.org/10.1016/j.soilbio.2018.07.022.

Fang, H., Liu, G., Kearney, M., 2005. Georelational analysis of soil type, soil salt content, landform, and land use in the Yellow River Delta. China. Environ. Manage. 35, 72–83. https://doi.org/10.1007/s00267-004-3066-2.

Feng, K., Zhang, Y., He, Z., Ning, D., Deng, Y., 2019. Interdomain ecological networks between plants and microbes. Mol. Ecol. Resour. 19, 1565–1577. https://doi.org/10.1111/1755-0998.13081.

Feng, K., Peng, X., Zhang, Z., Gu, S., He, Q., Shen, W., Wang, Z., Wang, D., Hu, Q., Li, Y., Wang, S., Deng, Y., 2022. iNAP: an integrated network analysis pipeline for microbiome studies. iMeta, e13. https://doi.org/10.1002/imt2.13.

Feng, K., Wang, S., He, Q., Bonkowski, M., Bahram, M., Yergeau, E., Wang, Z., Peng, X., Wang, D., Li, S., Wang, Y., Ju, Z., Du, X., Yan, C., Gu, S., Li, T., Yang, X., Shen, W., Wei, Z., Hu, Q., Li, P., Zhu, Y., Lu, G., Qin, C., Zhang, G., Xiao, C., Yang, Y., Zhou, J., Deng, Y., 2024. CoBacFM: Core bacteria forecast model for global grassland pH dynamics under future climate warming scenarios. One Earth 7, 1275–1287. https://doi.org/10.1016/j.oneear.2024.06.002.

Freilich, M.A., Wieters, E., Broitman, B.R., Marquet, P.A., Navarrete, S.A., 2018. Species co-occurrence networks: can they reveal trophic and non-trophic interactions in ecological communities? Ecology 99, 690–699. https://doi.org/10.1002/ecy.2142.

Friedman, J., Alm, E.J., 2012. Inferring correlation networks from genomic survey data. PLoS Comput. Biol. 8, e1002687. https://doi.org/10.1371/journal.pcbi.1002687.

Garcia, M.O., Templer, P.H., Sorensen, P.O., Sanders DeMott, R., Groffman, P.M., Bhatnagar, J.M., 2020. Soil microbes trade-off biogeochemical cycling for stress tolerance traits in response to year-round climate change. Front. Microbiol. 11. https://doi.org/10.3389/fmicb.2020.00616.

Joshua E. Goldford, Nanxi Lu, Djordje Bajić, Sylvie Estrela, Mikhail Tikhonov, Alicia Sanchez Gorostiaga, Daniel Segrè, Pankaj Mehta, Alvaro Sanchez. 2018. Emergent simplicity in microbial community assembly. Science. 361, 469-474. doi:10.1126/science.aat1168.

Grimm, V., Wissel, C., 1997. Babel, or the ecological stability discussions: an inventory and analysis of terminology and a guide for avoiding confusion. Oecologia 109, 323–334. https://doi.org/10.1007/s004420050090.

Gu, S.S., Hu, Q.L., Cheng, Y., Bai, L., Liu, Z., Xiao, W., Gong, Z., Wu, Y., Feng, K., Deng, Y., Tan, L., 2019. Application of organic fertilizer improves microbial community diversity and alters microbial network structure in tea (Camellia sinensis) plantation soils. Soil Tillage Res. 195, 104356. https://doi.org/10.1016/j.still.2019.104356.

Guillou, L., Bachar, D., Audic, S., Bass, D., Berney, C., Bittner, L., Boutte, C., Burgaud, G., de Vargas, C., Decelle, J., del Campo, J., Dolan, J.R., Dunthorn, M., Edvardsen, B., Holzmann, M., Kooistra, W.H.C.F., Lara, E., Le Bescot, N., Logares, R., Mahé, F., Massana, R., Montresor, M., Morard, R., Not, F., Pawlowski, J., Probert, I., Sauvadet, A.-L., Siano, R., Stoeck, T., Vaulot, D., Zimmermann, P., Christen, R., 2012. The Protist Ribosomal Reference database (PR2): a catalog of unicellular eukaryote Small Sub-Unit rRNA sequences with curated taxonomy. Nucleic Acids Res. 41, D597–D604. https://doi.org/10.1093/nar/gks1160.

Guo, Y., Gu, S., Wu, K., Tanentzap, A.J., Yu, J., Liu, X., Li, Q., He, P., Qiu, D., Deng, Y., Wang, P., Wu, Z., Zhou, Q., 2023. Temperature-mediated microbial carbon utilization in China's lakes. Glob. Chang. Biol. 29, 5044–5061. https://doi.org/10.1111/gcb.16840.

Guo, Y., Gu, S., Tanentzap, A.J., Wang, P., Li, Q., Wu, K., He, P., Liu, X., Yu, J., Qiu, D., Wu, J., Zhang, Y., Bai, G., Lee, S.M.-Y., Wu, Z., Zhou, Q., 2024. Submerged macrophyte restoration enhanced microbial carbon utilization in shallow lakes. Sci. Total Environ. 934, 173357. https://doi.org/10.1016/j.scitotenv.2024.173357.

Han, G., Chu, X., Xing, Q., Li, D., Yu, J., Luo, Y., Wang, G., Mao, P., Rafique, R., 2015. Effects of episodic flooding on the net ecosystem CO_2 exchange of a supratidal wetland in the Yellow River Delta. J. Geophys. Res. Biogeosci. 120, 1506–1520. https://doi.org/10.1002/2015JG002923.

Hautier, Y., Seabloom, E.W., Borer, E.T., Adler, P.B., Harpole, W.S., Hillebrand, H., Lind, E.M., MacDougall, A.S., Stevens, C.J., Bakker, J.D., Buckley, Y.M., Chu, C., Collins, S.L., Daleo, P., Damschen, E.I., Davies, K.F., Fay, P.A., Firn, J., Gruner, D.S., Jin, V.L., Klein, J.A., Knops, J.M.H., La Pierre, K.J., Li, W., McCulley, R.L., Melbourne, B.A., Moore, J.L., O'Halloran, L.R., Prober, S.M., Risch, A.C., Sankaran, M., Schuetz, M., Hector, A., 2014. Eutrophication weakens stabilizing effects of diversity in natural grasslands. Nature 508, 521–525. https://doi.org/10.1038/nature13014.

Helbing, D., 2013. Globally networked risks and how to respond. Nature 497, 51–59. https://doi.org/10.1038/nature12047.

Hernandez, D.J., David, A.S., Menges, E.S., Searcy, C.A., Afkhami, M.E., 2021. Environmental stress destabilizes microbial networks. ISME J. 15, 1722–1734. https://doi.org/10.1038/s41396-020-00882-x.

Herren, C.M., McMahon, K.D., 2017. Cohesion: a method for quantifying the connectivity of microbial communities. ISME J. 11, 2426–2438. https://doi.org/10.1038/ismej.2017.91.

Jennerjahn, T.C., Mitchell, S.B., 2013. Pressures, stresses, shocks and trends in estuarine ecosystems – an introduction and synthesis. Estuar. Coast. Shelf Sci. 130, 1–8. https://doi.org/10.1016/j.ecss.2013.07.008.

Jiao, N., Luo, T., Chen, Q., Zhao, Z., Xiao, X., Liu, J., Jian, Z., Xie, S., Thomas, H., Herndl, G.J., Benner, R., Gonsior, M., Chen, F., Cai, W.-J., Robinson, C., 2024. The microbial carbon pump and climate change. Nat. Rev. Microbiol. 22, 408–419. https://doi.org/10.1038/s41579-024-01018-0.

Jordán, F., 2009. Keystone species and food webs. Philos. Trans. R. Soc., B 364, 1733–1741. https://doi.org/10.1098/rstb.2008.0335.

Jousset, A., Bienhold, C., Chatzinotas, A., Gallien, L., Gobet, A., Kurm, V., Küsel, K., Rillig, M.C., Rivett, D.W., Salles, J.F., van der Heijden, M.G.A., Youssef, N.H., Zhang, X., Wei, Z., Hol, W.H.G., 2017. Where less may be more: how the rare biosphere pulls ecosystems strings. ISME J. 11, 853–862. https://doi.org/10.1038/ismej.2016.174.

Kang, H., Xue, Y., Cui, Y., Moorhead, D.L., Lambers, H., Wang, D., 2024. Nutrient limitation mediates soil microbial community structure and stability in forest restoration. Sci. Total Environ. 935, 173266. https://doi.org/10.1016/j.scitotenv.2024.173266.

Kong, Y., 2011. Btrim: a fast, lightweight adapter and quality trimming program for next-generation sequencing technologies. Genomics 98, 152–153. https://doi.org/10.1016/j.ygeno.2011.05.009.

Landi, P., Minoarivelo, H.O., Brännström, Å., Hui, C., Dieckmann, U., 2018. Complexity and stability of ecological networks: a review of the theory. Popul. Ecol. 60, 319–345. https://doi.org/10.1007/s10144-018-0628-3.

Li, J., Chen, Q., Li, Q., Zhao, C., Feng, Y., 2021a. Influence of plants and environmental variables on the diversity of soil microbial communities in the Yellow River Delta Wetland, China. Chemosphere. 274, 129967. https://doi.org/10.1016/j.chemosphere.2021.129967.

Li, S., Deng, Y., Du, X., Feng, K., Wu, Y., He, Q., Wang, Z., Liu, Y., Wang, D., Peng, X., Zhang, Z., Escalas, A., Qu, Y., 2021b. Sampling cores and sequencing depths affected the measurement of microbial diversity in soil quadrats. Sci. Total Environ. 767, 144966. https://doi.org/10.1016/j.scitotenv.2021.144966.

Li, S., Du, X., Feng, K., Wu, Y., He, Q., Wang, Z., Liu, Y., Wang, D., Peng, X., Zhang, Z., Escalas, A., Qu, Y., Deng, Y., 2022. Assessment of microbial α-diversity in one meter squared topsoil. Soil. Ecol. Lett. 4, 224–236. https://doi.org/10.1007/s42832-021-0111-5.

Liang, C., Schimel, J.P., Jastrow, J.D., 2017. The importance of anabolism in microbial control over soil carbon storage. Nat. Microbiol. 2, 17105. https://doi.org/10.1038/nmicrobiol.2017.105.

Ma, F., Wang, C., Zhang, Y., Chen, J., Xie, R., Sun, Z., 2022. Development of microbial indicators in ecological systems. Int. J. Environ. Res. Public Health 19, 13888. https://doi.org/10.3390/ijerph192113888.

MacArthur, R., 1955. Fluctuations of Animal Populations and a measure of Community Stability. Ecology 36, 533–536. https://doi.org/10.2307/1929601.

MacCallum, R.C., Browne, M.W., Sugawara, H.M., 1996. Power analysis and determination of sample size for covariance structure modeling. Psychol. Methods 1, 130–149. https://doi.org/10.1037/1082-989x.1.2.130.

Magoc, T., Salzberg, S.L., 2011. FLASH: fast length adjustment of short reads to improve genome assemblies. Bioinformatics 27, 2957–2963. https://doi.org/10.1093/bioinformatics/btr507.

Männistö, M., Ganzert, L., Tiirola, M., Häggblom, M.M., Stark, S., 2016. Do shifts in life strategies explain microbial community responses to increasing nitrogen in tundra soil? Soil Biol. Biochem. 96, 216–228. https://doi.org/10.1016/j.soilbio.2016.02.012.

Marsh, H.W., Hocevar, D., 1985. Application of confirmatory factor analysis to the study of self-concept: First- and higher order factor models and their invariance across groups. Psychol. Bull. 97, 562–582. https://doi.org/10.1037/0033-2909.97.3.562.

May, R.M., 1973. Stability and complexity in model ecosystems.

McDonald, R.P., Ho, M.H.R., 2002. Principles and practice in reporting structural equation analyses. Psychol. Methods 7, 64–82. https://doi.org/10.1037/1082-989x.7.1.64.

Michalet, R., Brooker, R.W., Cavieres, L.A., Kikvidze, Z., Lortie, C.J., Pugnaire, F.I., Valiente-Banuet, A., Callaway, R.M., 2006. Do biotic interactions shape both sides of the humped-back model of species richness in plant communities? Ecol. Lett. 9, 767–773. https://doi.org/10.1111/j.1461-0248.2006.00935.x.

Montesinos-Navarro, A., Hiraldo, F., Tella, J.L., Blanco, G., 2017. Network structure embracing mutualism–antagonism continuums increases community robustness. Nat. Ecol. Evol. 1, 1661–1669. https://doi.org/10.1038/s41559-017-0320-6.

Moore, J.C., McCann, K., de Ruiter, P.C., 2005. Modeling trophic pathways, nutrient cycling, and dynamic stability in soils. Pedobiologia 49, 499–510. https://doi.org/10.1016/j.pedobi.2005.05.008.

Murray, N.J., Phinn, S.R., DeWitt, M., Ferrari, R., Johnston, R., Lyons, M.B., Clinton, N., Thau, D., Fuller, R.A., 2019. The global distribution and trajectory of tidal flats. Nature 565, 222–225. https://doi.org/10.1038/s41586-018-0805-8.

Naeem, S., Thompson, L.J., Lawler, S.P., Lawton, J.H., Woodfin, R.M., 1994. Declining biodiversity can alter the performance of ecosystems. Nature 368, 734–737. https://doi.org/10.1038/368734a0.

Peng, X., Feng, K., Yang, X., He, Q., Zhao, B., Li, T., Wang, S., Deng, Y., 2024. iNAP 2.0: harnessing metabolic complementarity in microbial network analysis. iMeta 3, e235. https://doi.org/10.1002/imt2.235.

Pennekamp, F., Pontarp, M., Tabi, A., Altermatt, F., Alther, R., Choffat, Y., Fronhofer, E. A., Ganesanandamoorthy, P., Garnier, A., Griffiths, J.I., Greene, S., Horgan, K., Massie, T.M., Mächler, E., Palamara, G.M., Seymour, M., Petchey, O.L., 2018. Biodiversity increases and decreases ecosystem stability. Nature 563, 109–112. https://doi.org/10.1038/s41586-018-0627-8.

Piccardi, P., Vessman, B., Mitri, S., 2019. Toxicity drives facilitation between 4 bacterial species. PNAS 116, 15979–15984. https://doi.org/10.1073/pnas.1906172116.

Pimm, S.L., 1984. The complexity and stability of ecosystems. Nature 307, 321–326. https://doi.org/10.1038/307321a0.

Satorra, A., Bentler, P.M., 1988. Scaling Corrections for Statistics in Covariance Structure Analysis.

Schoch, C.L., Robbertse, B., Robert, V., Vu, D., Cardinali, G., Irinyi, L., Meyer, W., Nilsson, R.H., Hughes, K., Miller, A.N., Kirk, P.M., Abarenkov, K., Aime, M.C., Ariyawansa, H.A., Bidartondo, M., Boekhout, T., Buyck, B., Cai, Q., Chen, J., Crespo, A., Crous, P.W., Damm, U., De Beer, Z.W., Dentinger, B.T.M., Divakar, P.K., Dueñas, M., Feau, N., Fliegerova, K., García, M.A., Ge, Z.-W., Griffith, G.W., Groenewald, J.Z., Groenewald, M., Grube, M., Gryzenhout, M., Gueidan, C., Guo, L., Hambleton, S., Hamelin, R., Hansen, K., Hofstetter, V., Hong, S.-B., Houbraken, J., Hyde, K.D., Inderbitzin, P., Johnston, P.R., Karunarathna, S.C., Kõljalg, U., Kovács, G.M., Kraichak, E., Krizsan, K., Kurtzman, C.P., Larsson, K.-H., Leavitt, S., Letcher, P.M., Liimatainen, K., Liu, J.-K., Lodge, D.J., Jennifer Luangsa-ard, J., Lumbsch, H.T., Maharachchikumbura, S.S.N., Manamgoda, D., Martín, M.P., Minnis, A.M., Moncalvo, J.-M., Mulè, G., Nakasone, K.K., Niskanen, T., Olariaga, I., Papp, T., Petkovits, T., Pino-Bodas, R., Powell, M.J., Raja, H.A., Redecker, D., Sarmiento-

Ramirez, J.M., Seifert, K.A., Shrestha, B., Stenroos, S., Stielow, B., Suh, S.-O., Tanaka, K., Tedersoo, L., Telleria, M.T., Udayanga, D., Untereiner, W.A., Diéguez Uribeondo, J., Subbarao, K.V., Vágvölgyi, C., Visagie, C., Voigt, K., Walker, D.M., Weir, B.S., Weiß, M., Wijayawardene, N.N., Wingfield, M.J., Xu, J.P., Yang, Z.L., Zhang, N., Zhuang, W.-Y., Federhen, S., 2014. Finding needles in haystacks: linking scientific names, reference specimens and molecular data for Fungi. Database. 2014. 10.1093/database/bau061.

Schumacker, R.E., Lomax, R.G., 2004. A Beginner's Guide to Structural Equation Modeling: Fourth Edition (2nd ed.).

Shi, Z., Xu, X., Souza, L., Wilcox, K., Jiang, L., Liang, J., Xia, J., García-Palacios, P., Luo, Y., 2016. Dual mechanisms regulate ecosystem stability under decade-long warming and hay harvest. Nat. Commun. 7, 11973. https://doi.org/10.1038/ncomms11973.

Tanaka, J.S., Huba, G.J., 1985. A fit index for covariance structure models under arbitrary GLS estimation. Br. J. Math. Stat. Psychol. 38, 197–201. https://doi.org/10.1111/j.2044-8317.1985.tb00834.x.

Tilman, D., Downing, J.A., 1994. Biodiversity and stability in grasslands. Nature 367, 363–365. https://doi.org/10.1038/367363a0.

Tilman, D., Reich, P.B., Knops, J.M.H., 2006. Biodiversity and ecosystem stability in a decade-long grassland experiment. Nature 441, 629–632. https://doi.org/10.1038/nature04742.

Usman, M., Wang, M., Liu, Y., Li, L., Zhang, X., Xiao, T., Hou, F., 2025. High soil bacterial diversity increases the stability of the community under grazing and nitrogen. Soil Tillage Res. 248, 106414. https://doi.org/10.1016/j.still.2024.106414.

Waldrop, M.P., Firestone, M.K., 2006. Seasonal dynamics of microbial community composition and function in oak canopy and open grassland soils. Microb. Ecol. 52, 470–479. https://doi.org/10.1007/s00248-006-9100-6.

Wan, W., Tan, J., Wang, Y., Qin, Y., He, H., Wu, H., Zuo, W., He, D., 2020. Responses of the rhizosphere bacterial community in acidic crop soil to pH: changes in diversity, composition, interaction, and function. Sci. Total Environ. 700, 134418. https://doi.org/10.1016/j.scitotenv.2019.134418.

Wang, Q., Garrity, G.M., Tiedje, J.M., Cole, J.R., 2007. Naïve bayesian classifier for rapid assignment of rRNA sequences into the new bacterial taxonomy. Appl. Environ. Microbiol. 73, 5261–5267. https://doi.org/10.1128/AEM.00062-07.

Wu, M.H., Chen, S.Y., Chen, J.W., Xue, K., Chen, S.L., Wang, X.M., Chen, T., Kang, S.C., Rui, J.P., Thies, J.E., Bardgett, R.D., Wang, Y.F., 2021. Reduced microbial stability in the active layer is associated with carbon loss under alpine permafrost degradation. PNAS 118, e2025321118. https://doi.org/10.1073/pnas.2025321118.

Naijia Xiao, Aifen Zhou, Megan L. Kempher, Benjamin Y. Zhou, Zhou Jason Shi, Mengting Yuan, Xue Guo, Linwei Wu, Daliang Ning, Joy Van Nostrand, Mary K. Firestone, Jizhong Zhou. 2022. Disentangling direct from indirect relationships in association networks. Proc. Natl. Acad. Sci. U.S.A. 119, e2109995119. doi:10.1073/pnas.2109995119.

Yang, Z.p., Ou, Y.H., Xu, X.l., Zhao, L., Song, M.h., Zhou, C.p., 2010. Effects of permafrost degradation on ecosystems. Acta Pharmacol. Sin. 30, 33-39. Doi; 10.1016/j.chnaes.2009.12.006.

Yang, X., Feng, K., Wang, S., Yuan, M.M., Peng, X., He, Q., Wang, D., Shen, W., Zhao, B., Du, X., Wang, Y., Wang, L., Cao, D., Liu, W., Wang, J., Deng, Y., 2024. Unveiling the deterministic dynamics of microbial meta-metabolism: a multi-omics investigation of anaerobic biodegradation. Microbiome 12, 166. https://doi.org/10.1186/s40168-024-01890-1.

Yang, Z., Zhang, Q., Su, F., Zhang, C., Pu, Z., Xia, J., Wan, S., Jiang, L., 2017. Daytime warming lowers community temporal stability by reducing the abundance of dominant, stable species. Glob. Chang. Biol. 23, 154–163. https://doi.org/10.1111/gcb.13391.

Yarza, P., Yilmaz, P., Pruesse, E., Glöckner, F.O., Ludwig, W., Schleifer, K.H., Whitman, W.B., Euzéby, J., Amann, R., Rosselló Móra, R., 2014. Uniting the classification of cultured and uncultured bacteria and archaea using 16S rRNA gene sequences. Nat. Rev. Microbiol. 12, 635–645. https://doi.org/10.1038/nrmicro3330.

Yuan, M.M., Guo, X., Wu, L., Zhang, Y., Xiao, N., Ning, D., Shi, Z., Zhou, X., Wu, L., Yang, Y., Tiedje, J.M., Zhou, J., 2021. Climate warming enhances microbial network complexity and stability. Nat. Clim. Chang. 11, 343–348. https://doi.org/10.1038/s41558-021-00989-9.

Zaplata, M.K., Winter, S., Fischer, A., Kollmann, J., Ulrich, W., 2013. Species-driven phases and increasing structure in early-successional plant communities. Am. Nat. 181, E17–E27. https://doi.org/10.1086/668571.

Zelezniak, A., Andrejev, S., Ponomarova, O., Mende, D.R., Bork, P., Patil, K.R., 2015. Metabolic dependencies drive species co-occurrence in diverse microbial communities. PNAS 112, 6449–6454. https://doi.org/10.1073/pnas.1421834112.

Zelikova, T.J., Blumenthal, D.M., Williams, D.G., Souza, L., LeCain, D.R., Morgan, J., Pendall, E., 2014. Long-term exposure to elevated CO_2 enhances plant community stability by suppressing dominant plant species in a mixed-grass prairie. PNAS 111, 15456–15461. https://doi.org/10.1073/pnas.1414659111.

Zhang, G., Bai, J., Tebbe, C.C., Zhao, Q., Jia, J., Wang, W., Wang, X., Yu, L., 2021. Salinity controls soil microbial community structure and function in coastal estuarine wetlands. Environ. Manag. 23, 1020–1037. https://doi.org/10.1111/1462-2920.15281.

Zhao, M., Han, G., Wu, H., Song, W., Chu, X., Li, J., Qu, W., Li, X., Wei, S., Eller, F., Jiang, C., 2020. Inundation depth affects ecosystem CO_2 and CH_4 exchange by changing plant productivity in a freshwater wetland in the Yellow River Estuary. Plant and Soil 454, 87–102. https://doi.org/10.1007/s11104-020-04612-2.

Jizhong Zhou, Ye Deng, Feng Luo, Zhili He, Qichao Tu, Xiaoyang Zhi, David A. Relman. 2010. Functional Molecular Ecological Networks. mBio. 1, e00169-00110. 10.1128/mBio.00169-10.

Zhou, J., Xue, K., Xie, J., Deng, Y., Wu, L., Cheng, X., Fei, S., Deng, S., He, Z., Van Nostrand, J.D., Luo, Y., 2012. Microbial mediation of carbon-cycle feedbacks to climate warming. Nat. Clim. Chang. 2, 106–110. https://doi.org/10.1038/nclimate1331.